Charge susceptibility in the *t-J* model

D. N. Aristov[1,2,][*] and G. Khaliullin[1]

[1]*Institut für Theorie der Kondensierten Materie, Universität Karlsruhe, 76128 Karlsruhe, Germany*
[2]*Max-Planck-Institut für Festkörperforschung, Heisenbergstrasse 1, 70569 Stuttgart, Germany*
(Received 7 March 2006; revised manuscript received 4 May 2006; published 25 July 2006)

Momentum and doping dependence of the static charge susceptibility $\chi(\mathbf{q})$ in the t-t'-J model is investigated. Correlations lead to a strongly momentum-dependent renormalization of $\chi(\mathbf{q})$. The charge susceptibility near the (π,π) region of the Brillouin zone is strongly suppressed as the hole density δ is decreased. However, contrary to naive expectations, $\chi(\mathbf{q})$ around $\mathbf{q}=(\pi,0)$ and $(0,\pi)$ remains large and practically unchanged at $\delta \sim 0.1$–0.5. This effect is consistent with a tendency towards low-energy charge fluctuations with the wave vectors along the Γ-X direction, reported in earlier studies. Our main finding is that the above trends are amplified by J-driven pairing effects, indicating that the pseudogap formation may promote the charge inhomogeneity. The next-nearest hopping t' leads to weakening of the above momentum-selective renormalizations of $\chi(\mathbf{q})$. We analyze the effects of long-range Coulomb interaction, taking into account a layered structure of cuprates. As an application, the results are discussed in the context of bond-stretching phonon softening in hole-doped cuprates. In particular, a peculiar doping and momentum dependence of the electron-phonon coupling constant is found.

I. INTRODUCTION

Low-energy charge fluctuations and charge ordering becomes a hot topic in cuprates. Spatial modulation of the electronic states related to the local charge and/or bond ordering has been reported (see Ref. 1 and references therein). Indirect evidence for the low-energy charge dynamics is obtained from phonon anomalies induced by hole doping in cuprates.[2–4] These experiments motivate a theoretical study of the charge susceptibility in correlated models. In general, one expects an overall suppression of the electronic density fluctuations, hence the related charge susceptibility, as one approaches the Mott insulating limit by removing the doped holes. On the other hand, it is also known that correlations may promote low-energy charge instabilities—e.g, so-called stripe physics in cuprates and other oxide materials. These seemingly opposite trends indicate that the renormalization of the charge susceptibility by strong correlations is a quite subtle process.

Previous work on a charge response in the *t-J* (Refs. 5–7) and Hubbard models[8] focused mostly on finite frequency charge response, $\chi''(\omega,\mathbf{q})$, and on its frequency-integrated value, i.e., a structure factor $N(\mathbf{q})$. These quantities provide important information on electron-density fluctuation spectrum. In particular, Ref. 7 presented detailed calculations of $\chi''(\omega,\mathbf{q})$ within a slave-boson framework. A nontrivial momentum structure of low-energy excitations has been found. Dressing of the doped holes by underlying spin excitations—a phenomenon well known in the context of a magnetically ordered phase of *t-J* model—has also been captured within the $1/N$ expansion method for spin-disordered state. The results of Ref. 7 are in very good agreement with numerical data.[9,10]

Surprisingly, a static charge susceptibility $\chi_{\mathbf{q}}=\chi'(\omega=0,\mathbf{q})$ has escaped attention. To our knowledge, no detailed discussion of the momentum and doping dependence of $\chi_{\mathbf{q}}$ in the *t-J* model has thus far been reported. Meanwhile, this quantity which corresponds to the finite momentum compressibility contains important information, e.g, about potential charge instabilities. The aim of this paper is to fill this gap.

Specifically, we calculate $\chi(\mathbf{q})$ in the t-t'-J model and discuss the doping and spin-pairing effects on $\chi(\mathbf{q})$. Consistent with known results, we observe that correlations may drive phase separation at small doping, which is, however, eliminated by long-range Coulomb forces. Thus the charge instabilities, if any, are expected at intermediate or large wave vectors. For large momenta, we find that the correlation effects are highly anisotropic in a momentum space. While $\chi(\mathbf{q})$ is suppressed by a "hole-dilution" effect at certain parts of the Brillouin zone, it could even be enhanced for $\mathbf{q}$ along the Γ-X direction [from $q=0$ to $(\pi,0)$ or $(0,\pi)$]. As a result, a featureless charge susceptibility $\chi^{(0)}(\mathbf{q}) \sim$ const of noninteracting electrons obtains a strong momentum dependence. Physically, these observations originate from a nontrivial momentum structure of low-energy charge excitations found in Refs. 7, 9, and 10.

The main focus of the paper is to investigate how the above features in $\chi(\mathbf{q})$ are affected by the J term which induces a pseudogap in the fermionic dispersion. Formally, this is done by considering fluctuations in the density channel taking into account also the pairing fluctuations due to J interaction. We find that the pairing effects cooperate with a Gutzwiller constraint and enhance its momentum-selective renormalization of $\chi(\mathbf{q})$. Another issue, raised in our study, is the influence of the next-to-nearest neighbor hopping t', which is shown to somewhat weaken the above anomalies in $\chi(\mathbf{q})$. We also address a question of how the momentum dependence of the compressibility is changed by the Coulomb interaction. We provide a realistic treatment of the Coulomb potential accounting both for its long-range character and for the layered lattice structure of cuprates.

There have been a number of discussions in literature on how the correlations renormalize electron-phonon

coupling.[11–18] In Holstein-Hubbard type models (relevant to the problem of oxygen vibrations coupled to the electron-density) it was found that a peculiar "forward-scattering feature" may develop due to correlations. We will discuss a connection between this observation and our findings for the charge susceptibility $\chi(\mathbf{q})$. Related to this issue is the bond-stretching phonon anomalies in cuprates, which are discussed in the last part of this paper. This part extends the previous study[19,20] of the phonon-softening problem by including the pairing and t' effects.

The rest of the paper is organized as follows. Section II describes the formalism and discusses $\chi(\mathbf{q})$ in the t-only model. Sections III and IV focus on the effects of J and t' terms, correspondingly. In Sec. V, we derive a momentum dependence of Coulomb potential in the layered lattice structure, and calculate $\chi(\mathbf{q})$ at the presence of these interactions. The last section, Sec. VI, discusses renormalization of the electron-phonon coupling by correlations.

II. MODEL AND FORMALISM

The t-J Hamiltonian is

$$\mathcal{H} = -\sum_{ij} t_{ij} \tilde{c}_{i\sigma}^\dagger \tilde{c}_{j\sigma} - \mu \sum_i n_i + J \sum_{\langle ij \rangle} \left(\mathbf{s}_i \mathbf{s}_j - \frac{1}{4} n_i n_j \right) + \sum_{\langle ij \rangle} V_{ij} n_i n_j. \quad (1)$$

One of the useful approaches in treating the local constraint on the fermion occupation number, $\sum_\sigma c_{i\sigma}^\dagger c_{i\sigma} \le 1$, is the slave-boson representation $\tilde{c}_{i\sigma} = f_{i\sigma} b_i^\dagger$. The above inequality is then replaced by the constraint $b_i^\dagger b_i + \sum_\sigma f_{i\sigma}^\dagger f_{i\sigma} = N/2$, with the physical case of $N=2$. It is convenient also to consider the limit of the large number of spin indices (flavors), $N \gg 1$, since calculations are simplified this way (see, e.g., Ref. 5 and references therein).

Formally, the slave-boson approach implements the constraint of no double occupancy at the operator level. In the large-N limit, the mean number of bosons $\langle b_i^\dagger b_i \rangle$ is large and bosonic amplitude contains a large c-number component, a bosonic condensate. It was noted however, that the phase of each slave boson is a gauge degree of freedom, which is eliminated from the action by promoting the local Lagrange multipliers into time-dependent fields. The remaining degree of freedom for slave bosons is their real-valued amplitude, $b_j = r_j e^{i\varphi_j} \to r_j$ and one can formulate the "radial-gauge" representation for slave bosons.

Below we show how the leading-order results obtained for the charge susceptibility in the large-N slave-boson approach[5,7] can be reproduced in a simple manner. To clarify our approach, we let $J=0$ first, so that only a hopping term is present. We represent the constrained fermions as

$$\tilde{c}_{i\sigma}^\dagger = c_{i\sigma}^\dagger \sqrt{1 - n_i}, \quad (2)$$

with n_i the fermion occupation number, $n_i = \sum_\sigma c_{i\sigma}^\dagger c_{i\sigma}$.

We are interested in the charge susceptibility of the system, therefore we consider small fluctuations of the fermionic density n_i around its uniform equilibrium value $\bar{n}$. We expand the hopping term up to the second order in

$$\phi_i \equiv \delta n_i / 2 = (n_i - \bar{n})/2,$$

with the factor 2 introduced for later convenience;

$$\mathcal{H}_t = -\sum_{ij} t_{ij} c_{i\sigma}^\dagger \left[(1 - \bar{n}) - (\phi_i + \phi_j) - \frac{(\phi_i - \phi_j)^2}{2(1 - \bar{n})} \right] c_{j\sigma}. \quad (3)$$

In the Fourier representation, the first term above becomes a fermionic dispersion with the renormalized amplitude; the second term describes the scattering of the fermions on the fluctuations of density. The third term has a more complicated structure; for our purposes it is enough to consider its part, which is diagonal in fermionic momenta, $\propto c_{k1,\sigma}^\dagger c_{k2,\sigma}$ with $k_1 = k_2$. Then we write

$$\mathcal{H}_t \simeq \sum_{k\sigma} \xi_k c_{k\sigma}^\dagger c_{k\sigma} + \sum_{k,q,\sigma} (t_k + t_{k+q}) c_{k\sigma}^\dagger c_{k+q,\sigma} \phi_q$$

$$+ \sum_{kq\sigma} \frac{t_k - t_{k+q}}{1 - \bar{n}} c_{k\sigma}^\dagger c_{k\sigma} \phi_q \phi_{-q} \quad (4)$$

with

$$\xi_k = -(1 - \bar{n}) t_k + \mu, \quad (5)$$

$$t_k = 2t(\cos k_x + \cos k_y) - 4t' \cos k_x \cos k_y, \quad (6)$$

henceforth we set $t=1$. The constraint for n_i to be a number of on-site electrons leads to the appearance of the local Lagrange multipliers in the action

$$-\mu_q \left(2\phi_{-q} - \sum_{k,\sigma} c_{k\sigma}^\dagger c_{k+q,\sigma} \right),$$

so that the scattering term takes the form

$$\sum_{k,q} U_{kq} c_{k\sigma}^\dagger c_{k+q,\sigma}, \quad (7)$$

with $U_{kq} \equiv \phi_q(t_k + t_{k+q}) + \mu_q$. The average number of fermions is defined by $\bar{n} = 2\sum_k n_F(\xi_k)$ with $n_F(x)$ the Fermi factor. One can integrate out the fermions now, and obtain the effective low-energy action,

$$\mathcal{F}_t \simeq \sum_q [\phi_q \phi_{-q}(\omega_q - \Pi_2) - 2\phi_q \mu_{-q}(\Pi_1 + 1) - \mu_q \mu_{-q} \Pi_0], \quad (8)$$

$$\omega_q = 2\sum_k \frac{t_k - t_{k+q}}{1 - \bar{n}} n_F(\xi_k), \quad (9)$$

$$\Pi_n = \sum_k \frac{(t_k + t_{k+q})^n}{\xi_{k+q} - \xi_k} [n_F(\xi_k) - n_F(\xi_{k+q})]. \quad (10)$$

Requiring the zero variation, $\delta\mathcal{F}_t / \delta\mu_q = 0$, we determine the values of Lagrange multipliers

$$\mu_q = -\phi_q(1 + \Pi_1)/\Pi_0. \quad (11)$$

Inserting these values into Eq. (8), and recalling that $\phi_q = n_q/2$ at $q \ne 0$, we find

$$\mathcal{F}_t \simeq \sum_q \frac{n_q n_{-q}}{4}\left[\omega_q - \Pi_2 + \frac{(1+\Pi_1)^2}{\Pi_0}\right]. \qquad (12)$$

The above equation for the free energy in the harmonic approximation should be compared to the general expression $\mathcal{F} = \Sigma_q (2\chi_q)^{-1} n_q n_{-q} + \cdots$ with the static charge susceptibility χ_q. The value of χ_q as determined from Eq. (12) coincides with the result of Ref. 7 in the limit of $\omega = 0$ [however, a so-called polaron correction due to the higher $1/N$ term[7] is absent in Eq. (12)].

Let us first qualitatively analyze the above formula for the charge susceptibility. We introduce the doping level, or the concentration of holes,

$$\delta \equiv 1 - \bar{n},$$

and extract this factor from the dispersion ξ_q and the chemical potential μ,

$$\xi_{\mathbf{q}} = (-t_k + \tilde{\mu})\delta = \xi_{\mathbf{q}}^{(0)}\delta. \qquad (13)$$

Note that $\tilde{\mu}$ is positive and proportional to the doping level at $t' = 0$.

After some straightforward rearrangements of Eq. (12), the expression for $\chi(\mathbf{q})$ can be represented in the following form:

$$\chi_{\mathbf{q}} = \chi_{\mathbf{q}}^{(0)} \frac{\delta}{(\delta - \alpha_{\mathbf{q}})^2 + 2(\tilde{\mu}\delta + \beta_{\mathbf{q}})\chi_{\mathbf{q}}^{(0)}}. \qquad (14)$$

Bare quantities $\chi_{\mathbf{q}}^{(0)}$, $\alpha_{\mathbf{q}}$, and $\beta_{\mathbf{q}}$ are given in terms of the "noninteracting" dispersion $\xi_k^{(0)}$ as follows:

$$\chi_{\mathbf{q}}^{(0)} = 2\sum_k \frac{1}{\xi_{k+q}^{(0)} - \xi_k^{(0)}}[n_F(\xi_k^{(0)}) - n_F(\xi_{k+q}^{(0)})], \qquad (15)$$

corresponding to the bare susceptibility, and

$$\alpha_{\mathbf{q}} = \sum_k \frac{\xi_{k+q}^{(0)} + \xi_k^{(0)}}{\xi_{k+q}^{(0)} - \xi_k^{(0)}}[n_F(\xi_k^{(0)}) - n_F(\xi_{k+q}^{(0)})], \qquad (16)$$

$$\beta_{\mathbf{q}} = -\sum_k \frac{\xi_{k+q}^{(0)}\xi_k^{(0)}}{\xi_{k+q}^{(0)} - \xi_k^{(0)}}[n_F(\xi_k^{(0)}) - n_F(\xi_{k+q}^{(0)})]. \qquad (17)$$

One can show that the function $\beta_{\mathbf{q}}$ in Eq. (17) is positive. Equation (14) should be understood as a renormalization of the charge susceptibility by correlation effects $\chi_{\mathbf{q}}/\chi_{\mathbf{q}}^{(0)} = G_{\mathbf{q}}(\delta)$ where a function $G_{\mathbf{q}}(\delta)$ is given by a fraction in Eq. (14). This momentum and doping dependent factor results from the action of the Gutzwiller constraint in the density channel. Whereas a noninteracting susceptibility $\chi_{\mathbf{q}}^{(0)}$ is a featureless function in the absence of nesting (at $\delta = 0$, $t' = 0$), the correlation effects bring a pronounced momentum structure in $\chi_{\mathbf{q}}$ via the function $G_{\mathbf{q}}(\delta)$.

At large doping levels, $G_{\mathbf{q}}(\delta)$ eventually approaches unity. The action of this factor at small doping is highly momentum-selective. Inspecting Eqs. (14)–(17) at $t' = 0$, one finds that $G_{\mathbf{q}}(\delta) \propto \delta$ for $\mathbf{q} \sim (\pi, \pi)$ (with omitted logarithmic corrections). This is simply understood as a reduction of density fluctuations due to a removal of the holes. (Alternatively, one may say, that the checkerboard structure in positions of
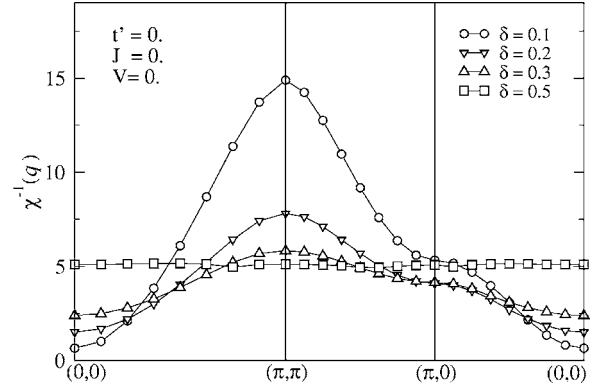

FIG. 1. The inverse nonuniform compressibility calculated for the tight-binding spectrum.

small amount of doped holes is the least energetically favorable.) At small momenta, however, the effect is opposite and one has $G_{\mathbf{q}}(\delta) \propto 1/\delta$. This means a divergent compressibility as one approaches the Mott limit, in accordance with previous studies of Hubbard[21] and *t-J* models,[22–24] and reflects a well-known tendency towards phase separation.[25–27] Competition between these two effects—a hole dilution and phase separation—leads to a nontrivial momentum structure. It is interesting to note that this structure is complementary to that in the spin sector, where correlations enhance the spin susceptibility at $\mathbf{q} \sim (\pi, \pi)$,[26,28] but not at small momenta.

These qualitative observations are further illustrated by the numerical calculations. In Fig. 1, we show the momentum dependence of $\chi_{\mathbf{q}}$ along the symmetry lines in the Brillouin zone. The above behavior of $\chi_{\mathbf{q}}$ with doping is clearly visible at the symmetry points. In order to emphasize this nontrivial momentum dependence induced by the Gutzwiller constraint, we plot $\chi_{\mathbf{q}}/\chi_{\mathbf{q}}^{(0)} = G_{\mathbf{q}}(\delta)$ in Fig. 2 for several dopings $\delta \simeq (0.1, 0.2, 0.3, 0.5)$. To see the doping dependence in more detail, we show $\chi_{\mathbf{q}}$ in Fig. 3 as a function of doping at three symmetry points $\mathbf{q} = 0$, $(\pi, 0)$, and (π, π). One observes that the curves for $\chi_{\mathbf{q}} \neq 0$ eventually turn down at small doping δ. Remarkably, the value of $\chi_{\mathbf{q}}$ at $(\pi, 0)$ upon decreasing δ is somewhat enhanced before the downward turn, which shows the competition between two trends: phase separation and hole dilution.
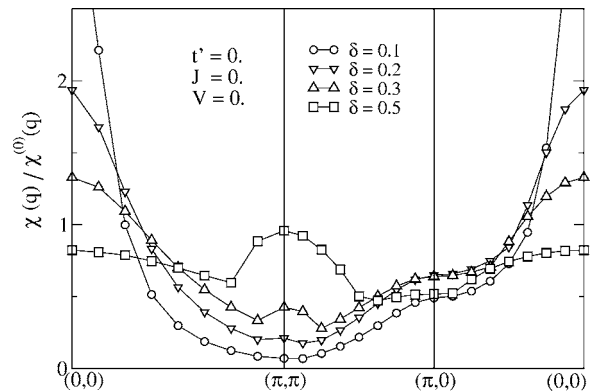

FIG. 2. Renormalization of the susceptibility due to the Gutzwiller constraint.
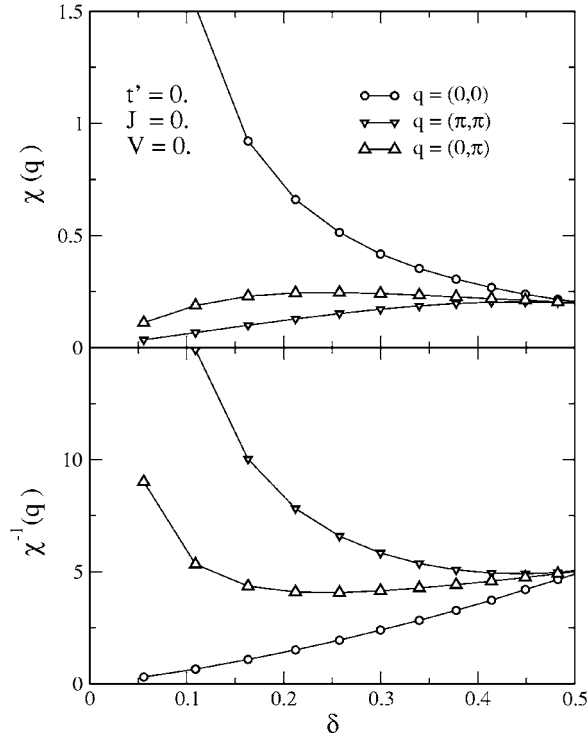
FIG. 3. Doping dependence of the charge susceptibility (upper panel) and its inverse value (lower panel) at the symmetry points.

Small momentum anomalies are eliminated in reality by Coulomb repulsion. A detailed study of this problem is presented in Sec. V. We show there that a pronounced momentum structure of $\chi(\mathbf{q})$ with very different doping dependence at (π,π) and $(\pi,0)$ regions still remains at the presence of Coulomb interactions.

III. J TERM: PSEUDOGAP EFFECTS

We consider now how the above observations change at the presence of pseudogap effects induced by the J term in the Hamiltonian. In the spirit of large-N slave-boson theories, we refer to pseudogap as a fermionic gap arising from mean-field decoupling of the superexchange interaction in the pairing channel. A question addressed here is that of how such a gap and fluctuations of the pairing field around a uniform mean-field solution will affect the charge susceptibility.

The four-fermion J term can be represented in the form

$$\mathcal{H}_J = -\frac{1}{2} \sum_{k_1,k_2,k_3} c_{k_1,\uparrow}^\dagger c_{k_2,\downarrow}^\dagger c_{k_3,\downarrow} c_{k_4,\uparrow} (J_{k_4-k_1} + J_{k_3-k_1}) \quad (18)$$

with $k_4 = k_1 + k_2 - k_3$ and the nearest-neighbor interaction $J_k = 2J(\cos k_x + \cos k_y)$. Introducing the quantity

$$\eta_q^\pm = \sum_k c_{k+q/2,\downarrow} c_{-k+q/2,\uparrow} \gamma_k^\pm, \quad (19)$$

with

$$\gamma_k^\pm = (\cos k_x \pm \cos k_y)/2, \quad (20)$$

we represent the J term as

$$\mathcal{H}_J = -4J \sum_{q,\alpha=\pm} (\eta_q^\alpha)^\dagger \eta_q^\alpha. \quad (21)$$

This expression can be decoupled by the Hubbard-Stratonovich transformation as follows:

$$\mathcal{H}_J = \sum_{q,\pm} \left[(d_q^\pm \eta_q^\pm + \text{H.c.}) + \frac{|d_q^\pm|^2}{4J} \right]. \quad (22)$$

Here d_q^- and d_q^+ stand for the amplitudes of the d-wave and extended s-wave pairing, respectively, in the channel with nonzero total momentum, q. The total Hamiltonian is then quadratic in fermions, which interact with the fluctuations ϕ_q, μ_q, and $d_q^\pm$.

We assume that the d-wave pairing sets in, which corresponds to the nonzero value of the order parameter $d_0^- \equiv \Delta$. The spectrum is given by $\varepsilon_k^2 = \xi_k^2 + \Delta_k^2$, where $\Delta_k = d_0^- \gamma_k^-$. The self-consistency gap equation in the small-coupling limit reads

$$1 = 2J \sum_k \frac{(\gamma_k^-)^2}{\varepsilon_k} \tanh \frac{\varepsilon_k}{2T}. \quad (23)$$

Restricting our consideration by the quadratic terms in the above nonuniform fluctuations, we would like to obtain an expression similar to Eq. (12), but in the presence of the pairing. After some standard analysis, we arrive at the bosonic-type action of the form

$$\mathcal{F}_{t-J} = \sum_q \Phi_q^\dagger M_q \Phi_q, \quad (24)$$

$$\Phi_q^\dagger = (\phi_q, \mu_q, d_q^+, d_q^-), \quad (25)$$

with the matrix

$$M_q = \begin{pmatrix} \omega_q - \Pi_2 & -1 - \Pi_1 & A_1^+ & A_1^- \\ -1 - \Pi_1 & -\Pi_0 & A_0^+ & A_0^- \\ A_1^+ & A_0^+ & (4J)^{-1} - D_{ss} & -D_{sd} \\ A_1^- & A_0^- & -D_{sd} & (4J)^{-1} - D_{dd} \end{pmatrix}. \quad (26)$$

Here in the low-temperature limit

$$\omega_q = \sum_k \frac{t_k - t_{k+q}}{1 - \bar{n}} \frac{\varepsilon_k - \xi_k}{\varepsilon_k},$$

$$\Pi_n = \sum_k (t_+ + t_-)^n \frac{\varepsilon_+ \varepsilon_- - \xi_+ \xi_- + \Delta_+ \Delta_-}{2\varepsilon_+ \varepsilon_- (\varepsilon_+ + \varepsilon_-)}, \quad (27)$$

$$\begin{pmatrix} A_n^+ \\ A_n^- \end{pmatrix} = \sum_k (t_+ + t_-)^n \frac{\Delta_+ \xi_- + \xi_+ \Delta_-}{2\varepsilon_+ \varepsilon_- (\varepsilon_+ + \varepsilon_-)} \begin{pmatrix} \gamma_k^+ \\ \gamma_k^- \end{pmatrix}, \quad (28)$$

and

$$\begin{pmatrix} D_{ss} \\ D_{sd} \\ D_{dd} \end{pmatrix} = \sum_k \frac{\varepsilon_+ \varepsilon_- - \xi_+ \xi_-}{2\varepsilon_+ \varepsilon_- (\varepsilon_+ + \varepsilon_-)} \begin{pmatrix} [\gamma_k^+]^2 \\ \gamma_k^- \gamma_k^+ \\ [\gamma_k^-]^2 \end{pmatrix}, \quad (29)$$

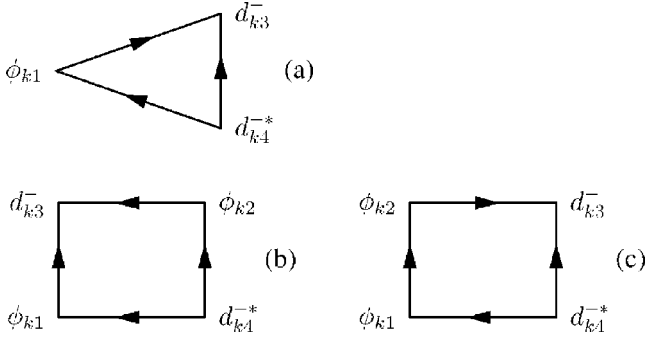and we used the shorthand notation $\xi_\pm = \xi_{k \pm q/2}$, $\varepsilon_\pm = \varepsilon_{k \pm q/2}$, etc.

FIG. 4. Multitail fermionic Feynman diagrams, leading to higher-order terms in the bosonic action. Fermionic Green functions are shown by lines with arrows; bosonic fields ϕ, d^- stand in the vertices. For simplicity we do not show the internal momenta.

We are interested in the charge susceptibility, which should basically be determined by integrating out the pairing fluctuations in Eq. (25) and setting the Lagrange multipliers μ_q to their saddle-point values. Both steps are essentially the same for the quadratic action, so that the needed compressibility is given by the upper left element of the inverse matrix M_q, namely,

$$\chi_q = 2[M_q^{-1}]_{11}. \tag{30}$$

Let us briefly discuss here how the intersite Coulomb interaction V_{ij} is included in our formalism. We write it in the form $\Sigma_{\langle ij \rangle} V_{ij}(n_i - \bar{n})(n_j - \bar{n}) = \frac{1}{2}\Sigma_q V_q n_q n_{-q} = 2\Sigma_q V_q \phi_q \phi_{-q}$, and see that this interaction modifies the only matrix element in Eq. (26), so that

$$[M_q]_{11} \rightarrow \omega_q - \Pi_2 + 2V_q. \tag{31}$$

The last equation shows that we treat the interaction V_q within the random-phase approximation (RPA) scheme. It can also be shown that

$$\chi_{V,q}^{-1} = \chi_{V=0,q}^{-1} + V_q, \tag{32}$$

i.e., one can calculate χ_q at $V_q=0$, and include $V_q \neq 0$ afterwards. At the same time, the inclusion of $V_q \neq 0$ should be done from the beginning for the calculation of d-wave susceptibility $\chi_{dd}(\mathbf{q})$ (see below).

It is also worth noting that in the absence of pairing, $\Delta_k \equiv 0$, the coefficients $D_{\alpha\beta}$ in Eq. (26) remain finite, and $A_n^{\pm}$ vanish. It means that in the harmonic approximation the superconducting-type fluctuations affect the charge susceptibility only at finite Δ. At the same time, in more general treatment, the superconducting fluctuations $d^{\pm}$ affect the density fluctuations in the higher orders even at $\Delta_k \equiv 0$. Considering multitail fermionic loops, one obtains, e.g., the terms in the bosonic action of the form

$$A_1^{--}\phi_{k_1}d_{k_2}^-d_{k_3}^{-*} + B^{--}\phi_{k_1}\phi_{k_2}d_{k_3}^-d_{k_4}^{-*},$$

etc., where the coefficients A_1^{--}, B^{--} are defined by the Feynman diagrams shown schematically in Figs. 4(a)–4(c), respectively. One can notice that the diagram in Fig. 4(b) corresponds to an analog of Maki-Thompson contribution to paraconductivity and the diagram in Fig. 4(c) reflects the
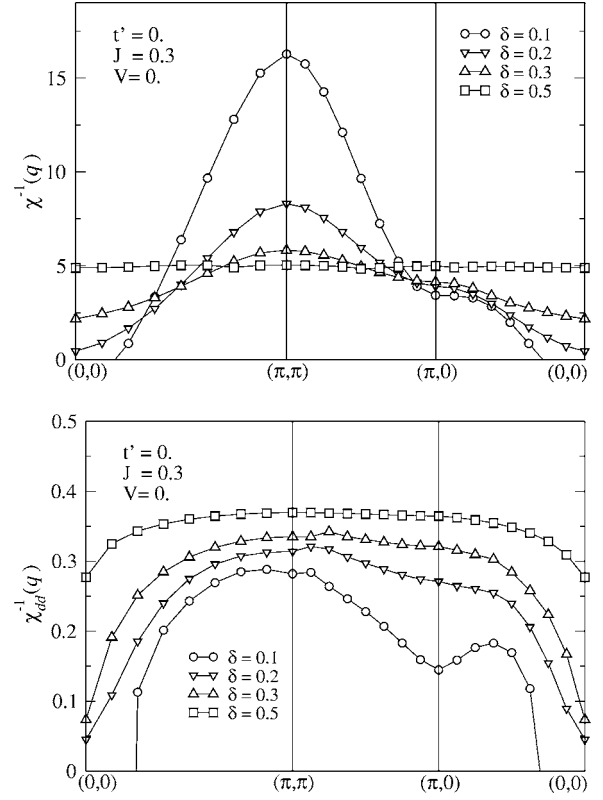

FIG. 5. Behavior of inverse charge (upper panel) and d-wave pair (lower panel) susceptibilities at $J=0.3$.

"density of states correction," see Ref. 29. The contribution of the diagram in Fig. 4(a) is zero at $\Delta_k \equiv 0$. However, in the presence of the pairing condensate, one external bosonic field d^- sets to a constant, contributing in the lowest order to the term A_1^- in Eq. (26), etc. The calculation of such fluctuation corrections to the charge susceptibility is clearly beyond the scope of the present study.

In our numerical calculations we set $J=0.3$, and determined Δ from the self-consistency equation (23) at $T=0$. One should note, that at $T=0$, Eq. (23) has a solution $\Delta \neq 0$ for any doping, although Δ can be exponentially small. In our calculation, we ruled out the solutions with $|\Delta| < 10^{-3}t$, thus implicitly setting the temperature to be very small but finite, $T \sim 10^{-3}t$. The matrix M is then found from Eqs. (27)–(29), and χ_q from Eq. (30).

The obtained results are shown in Fig. 5. Comparing the upper panel in Fig. 5 with the previous Fig. 1, we observe that χ_q is still rather flat in the whole Brillouin zone at large dopings. At smaller dopings the above momentum-selective features are enhanced by the pseudogap appearance, with somewhat increase of χ_q^{-1} at $\mathbf{q} = (\pi, \pi)$ and a new qualitative change at small wave vectors. Namely, the compressibility attains negative values at finite $\delta \sim 0.15$, which means that the Gaussian action $\sim \chi_q^{-1}(\delta n_q)^2$ is unstable in a rather extended range of dopings and the analysis of the next orders in δn_q is needed. This instability is accompanied by the divergence in the d-wave susceptibility χ_{dd} defined as the $\frac{1}{2}[M_q^{-1}]_{44}$, as is seen in the lower panel in Fig. 5. We remind the reader that the latter quantity is always positive χ_{dd}^{-1}

$\sim \Delta^2/t$ in the absence of feedback from density fluctuations to the superconducting ones, i.e., when $A_n^{\pm} \equiv 0$. The unstable pairing part of the action $\sim \Sigma_q \chi_{dd}^{-1}(\mathbf{q})|d_q^-|^2$ particularly means that the uniformly paired ground state determined by the gap equation (23) is no longer justified.

Our finding that J-pairing fluctuations and charge fluctuations grow up concomitantly could be understood as a dynamical modulation of pairing amplitude consistent with the results by Vojta *et al.*[30,31] It is also noticed that a dramatic enhancement of the charge susceptibility at small momenta due to the J term is consistent with previous reports (see, e.g., Fig. 3 of Ref. 26) that the superexchange interaction increases a tendency towards phase separation. Close to such instabilities, the higher-order terms (beyond the Gaussian action) should be included in the theory, which problem deserves a separate study.

IV. NEXT-NEAREST HOPPING

We discuss now the effects of next-to-nearest neighbor hopping t' which is present in cuprates and has in fact been suggested to be a key empirical parameter for superconductivity.[32] Effects of t' on physical quantities such as spin and fermionic excitations in the t-J model has been found to be substantial, see, e.g., Ref. 33. Concerning the charge compressibility, several studies found that t' hopping reduces a tendency towards phase separation.[26,34,35]

Consider first the qualitative effect of $t' \neq 0$ in the absence of the J term. Using Eq. (14), one can still show that the renormalization factor $G_{\mathbf{q}}(\delta) \sim \delta$ at $\mathbf{q}=(\pi,\pi)$. At the same time, for $t' \neq 0$ the chemical potential $\tilde{\mu}$ does not vanish when $\delta \to 0$ and we have finite $G_{\mathbf{q}}(\delta) \sim 1/\tilde{\mu}$ at small momenta. It means that finite (*positive*) t' reduces the tendency to the phase separation at small doping, consistent with previous work. It is interesting to note that the *negative* t' has an opposite effect. Indeed, in this case the chemical potential $\tilde{\mu}$ is also negative. By inspecting Eq. (14) one observes that this may lead to negative values of the susceptibility at small momenta and doping, indicating an instability of the uniform state for the $t' < 0$ case at small dopings.

We showed in the previous section that the inclusion of the J term drives the system closer to the instability point for charge fluctuations at $t'=0$, and the same thing should happen when next-to-nearest neighbor hopping is present. To verify it, we recalculated $\chi_{\mathbf{q}}$ for $t'=0.3$, $J=0.3$ for the same values of doping δ as above. The results are shown in Fig. 6. Comparing it to Fig. 5, one confirms that the finite next-nearest hopping $t'>0$ somewhat stabilizes the charge fluctuations. The comparison to Fig. 1 shows, however, that the effect of the J term is still dominant and χ_q is (nearly) divergent at $\delta=0.1$.

We should emphasize that the above statements on the role of t' and J terms do not explicitly rely on the one-particle properties of the spectrum, such as van Hove singularities and flat parts of dispersion around $(0,\pi)$ points. Our discussion includes two-particle Green's functions, both particle-hole and particle-particle fermionic loops, and the eventual integration over bosons in the effective action, i.e., obtaining Eq. (30) from Eq. (24), corresponds to the simul-
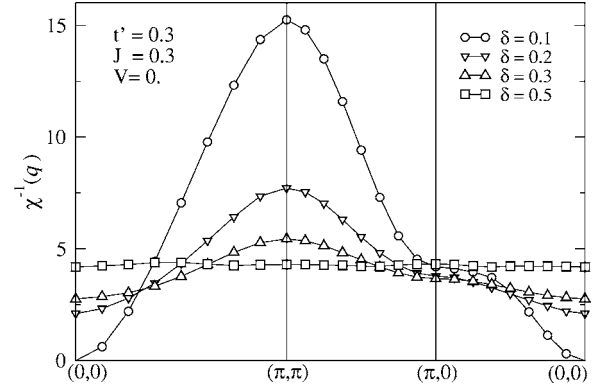

FIG. 6. Inverse charge susceptibility at $t'=0.3$ and $J=0.3$. Anomalies at small momenta seen in Fig. 5 are suppressed.

taneous resumming of the RPA series in both Gutzwiller and J-term channels.

Summarizing here, the static susceptibility shows no structure in the Brillouin zone at a large value of the hole doping, $\delta \simeq 0.5$. This could be expected for a system without strong correlations and with a large Fermi surface, since in the 2D Fermi gas, $\chi_q=$const at $q < 2k_F$. The flat shape of χ_q at large δ is rather insensitive to the values of the second hopping and pairing. At smaller dopings, χ_q demonstrates a pronounced structure in q-space; the tendency to long-scale phase separation is somewhat weakened by finite values of the second hopping, but the pairing fluctuations, induced by the J term, dominate and eventually make the system unstable both in charge and pairing channels.

V. LONG-RANGE COULOMB INTERACTION

Charge susceptibility is strongly influenced by a nonlocal repulsion between the holes. Quite often (in numerical studies in particular) these interactions are approximated by a nearest-neighbor potential V_1, which is already sufficient to observe the suppression of phase separation effects discussed above. We are, however, interested in a more detailed momentum dependence of χ_q. For this purpose, one has to use more realistic, i.e., long-range form of the Coulomb potential. We consider first its momentum dependence in a layered cuprate structure, taking into account a discrete nature of the lattice within the planes as well.

At small momenta, where no lattice structure is relevant, a continuum limit applies;

$$V_C(\mathbf{Q}) = \frac{4\pi e^2}{\epsilon_{ab}q^2 + \epsilon_c q_z^2}. \tag{33}$$

Here, ϵ_{ab} and ϵ_c are zero-frequency dielectric constants determined usually from optical data, and $q^2=q_x^2+q_y^2$. (a and b directions are assumed to have the same ϵ.) We use a notation $\mathbf{Q}=(\mathbf{q},q_z)$, with in-plane and out-of-plane components, $\mathbf{q}$ and q_z, respectively. For $q_z=0$, the above equation gives $V(\mathbf{q})=4\pi e^2/\epsilon_{ab}q^2$, a conventional three-dimensional (3D) potential. We recall that in two-dimensional (2D) (the case of infinitely separated planes) $V(\mathbf{q}) \propto 1/q$, and we discuss the crossover between these two regimes below.

We argue here that for our analysis it is possible to neglect a momentum dependence of the dielectric constants, because at low energy they are mostly contributed by (dispersionless) optical phonons and nearly localized, high-energy electronic processes. In this case the real space representation of Eq. (33), valid up to interatomic distances, reads as follows:

$$V_C(\mathbf{R}) = \frac{e^2}{\sqrt{\epsilon_{ab}\epsilon_c}} \frac{1}{[(\epsilon_{ab}/\epsilon_c)z^2 + r^2]^{1/2}}. \quad (34)$$

Here, r is a distance within the ab plane, and $R^2 = r^2 + z^2$. In the isotropic case $\epsilon_{ab} = \epsilon_c$, a familiar expression $e^2/\epsilon R$ follows from this equation.

Let us consider now a lattice with periodicity a within the planes and d along the c axis (in the La$_2$CuO$_4$ structure, d is a half of the c axis lattice parameter, i.e., $d = c/2$). We determine the Coulomb repulsion V_{ij} between the electrons, referring to the sites i and j. In our tight-binding situation the electronic wave functions are almost localized around the ith ion and their amplitude squared gives the density around this ion. We denote this density, or charge distribution function, by $f(\mathbf{R} - \mathbf{R}_i)$, and write

$$V_{ij} = \int d\mathbf{R}' d\mathbf{R}'' f(\mathbf{R}' - \mathbf{R}_i) f(\mathbf{R}'' - \mathbf{R}_j) V_C(\mathbf{R}' - \mathbf{R}'')$$

$$= \int \frac{d\mathbf{Q}}{(2\pi)^3} |f(\mathbf{Q})|^2 V_C(\mathbf{Q}) e^{i\mathbf{Q}(\mathbf{R}_i - \mathbf{R}_j)}, \quad (35)$$

where the integration is over the whole continuum and V_C is given by Eqs. (33) and (34) in a momentum and real spaces, respectively. The Fourier transform of V_{ij} then reads as

$$V(\mathbf{Q}) = \sum_{j \neq i} V_{ij} e^{i\mathbf{Q}(\mathbf{R}_i - \mathbf{R}_j)}$$

$$= \frac{1}{a^2 d} \sum_{\mathbf{G}_3} |f(\mathbf{Q} + \mathbf{G}_3)|^2 V_C(\mathbf{Q} + \mathbf{G}_3) - V_{ii} \quad (36)$$

with $\mathbf{G}_3$ the 3D wave vector of reciprocal lattice.

On the physical grounds, one expects that a doped hole (the Zhang-Rice singlet) is a rather extended object in the ab plane and nearly localized in this plane. A reasonable choice for a hole-shape function is

$$f(\mathbf{R}) = (\kappa^2/2\pi) e^{-\kappa r} \delta(z),$$

which decays at distances $1/\kappa$ in the plane. Physically, the size of the Zhang-Rice singlet should at least be about Cu-O distance, so $\kappa \sim 2/a$ might be a representative value. A momentum counterpart of the latter function

$$f(\mathbf{Q}) = (1 + q^2/\kappa^2)^{-3/2} \quad (37)$$

should then be understood as a form-factor of the Zhang-Rice singlet.

Given that the form-factor $f(\mathbf{Q})$ is independent of the q_z component, the summation over $G_z = 2\pi n/d$ ($n = 0, \pm 1, \pm 2, \ldots$) in Eq. (37) is easily performed for any q_z. The result for our primary case of interest $q_z = 0$ is

$$V_{\mathbf{q}} \equiv V(\mathbf{q}, 0) = \sum_{\mathbf{G}_2} |f(\mathbf{q} + \mathbf{G}_2)|^2 V^{(0)}(\mathbf{q} + \mathbf{G}_2) - V_{ii}, \quad (38)$$

where $\mathbf{G}_2 = 2\pi(n, m)/a$ is the reciprocal wave vector for a square lattice and

$$V^{(0)}(\mathbf{q}) = \frac{V}{qa \tanh(q/q_0)}, \quad (39)$$

$$V = \frac{2\pi e^2}{a\sqrt{\epsilon_{ab}\epsilon_c}}, \quad (40)$$

$$q_0 \equiv 2/\tilde{d} = (2/d)\sqrt{\epsilon_c/\epsilon_{ab}}. \quad (41)$$

Here $\tilde{d}$ is an effective interlayer distance. The potential (39) interpolates between 3D $Vq_0/q^2 a$ and 2D V/qa limits at small $q \ll q_0$ and large $q \gg q_0$ momenta, respectively. This crossover at q_0 reflects the fact that the planes are independent at large momenta. For an La$_2$CuO$_4$ compound where $\epsilon_c/\epsilon_{ab} \sim 1/2$,[36] the value of crossover momentum is estimated as $q_0 \simeq 0.8/a$.

The function (38) is explicitly periodic in q space. In the particular model for the form-factor, Eq. (37), the subtracted term V_{ii} is evaluated as $V_{ii} = 3\kappa a V/32$. In general, $V_{\mathbf{q}}$ is a sign-reversal function in the Brillouin zone, as it should be in view of $\Sigma_{\mathbf{Q}} V(\mathbf{Q}) = V(\mathbf{R} = 0) = 0$. In the case of a continuum limit for the planes[37] (instead of the tight-binding model used here), the Coulomb potential would be given solely by Eq. (39), the result formally obtained from Eq. (38) by setting $V_{ii} = 0$, $f(\mathbf{q}) = 1$ and taking the $\mathbf{G}_2 = 0$ term alone. Finally, we note for completeness that $V(\mathbf{q}, q_z)$ for arbitrary q_z is again given by Eq. (38) but the potential $V^{(0)}(\mathbf{q})$ for a continuum limit in Eq. (39) must be replaced by $V^{(0)}(\mathbf{q}, q_z) = V^{(0)}(\mathbf{q})/(1 + F_z^2)$, where $F_z = \sin(q_z d/2)/\sinh(q\tilde{d}/2)$.[37]

At moderate $\kappa \sim 1$ *and* small momenta $q < \kappa$ (or, alternatively, at distances exceeding the size of Zhang-Rice singlet), only the $\mathbf{G}_2 = 0$ term in Eq. (38) contributes and $V_{\mathbf{q}} \simeq V^{(0)}(\mathbf{q})$. The rapid decay of $|f(\mathbf{q})|^2$ [see Eq. (37)], cuts off the values of $V_{\mathbf{q}}$ at larger momenta $q \gtrsim \kappa$.

The opposite limit $\kappa a \gg 1$ corresponds to the point-charge approximation and the sum in Eq. (38) formally diverges with κ. This divergence is canceled by the above on-site term $V_{ii} \propto \kappa$. In the Appendix, we provide another representation for $V_{\mathbf{q}}$ in the point-charge limit; it works increasingly well for $\kappa a \gtrsim 3$.

Figure 7 shows $\mathbf{q}$ dependence of the Coulomb potential, Eq. (38), as a function of parameter κ at fixed $q_0 = 0.8/a$. $V_{\mathbf{q}}/V$ evolves from the point-charge limit with visible sign-reversal character to nearly positive curves as κ decreases. For comparison, we also show a frequently used simple short-range repulsion model

$$V_q = 2V_1(\cos q_x + \cos q_y) + 4V_2 \cos q_x \cos q_y$$

with $V_1 = V/2\pi$, $V_2 = V_1/\sqrt{2}$ (dashed-dotted line), and the result that would be obtained when the lattice structure is discarded within the planes (dotted line). The latter is always positive as should be for the charges in a continuum.
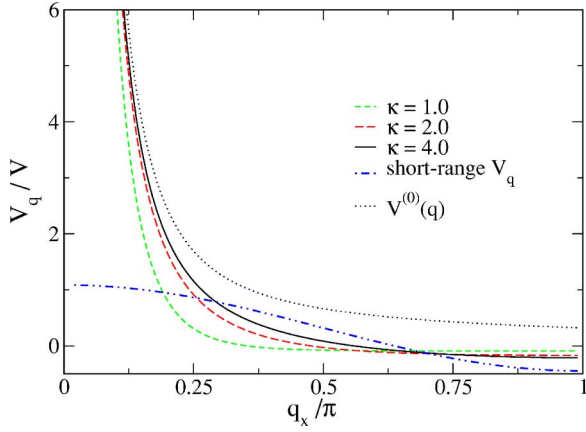
FIG. 7. (Color online) Coulomb potential $V_{\mathbf{q}}/V$ for different values of κ. A crossover momentum $q_0=0.8/a$. For comparison, a dashed-dotted line shows a simple model which includes nearest-neighbor (NN) and next-nearest-neighbor (NNN) repulsion only. The dotted line is calculated from Eq. (39) neglecting the lattice structure within the planes.

Let us turn now to the charge susceptibility and consider how it is influenced by long-range Coulomb interactions. First, we estimate the energy scale V in Eq. (40). Using a representative value $\sqrt{\epsilon_{ab}\epsilon_c}\sim30$,[36] one finds $V\simeq0.8$ eV, which is about 2 in units of t.[38] Second, we should in principle complement the Coulomb potential with short-range interactions between the holes, stemming from local physics. One such contribution is that of a well-known "missing J link," which gives NN attraction of the scale of $J\langle\mathbf{s}_i\mathbf{s}_j -1/4\rangle\sim-(0.1\div0.2)t$. Yet another local interaction is mediated by the bond-stretching vibration of an oxygen shared by the two NN holes. This contribution is repulsive at a low-energy limit because of the coupling geometry (see, for details, Sec. VI), and is given by a half of the polaron binding energy $E_b/2\sim t/4$ (estimated below from the phonon shift induced by doping). Altogether, these two local NN contributions of different sign tend to cancel each other and their small net result could be neglected. Hence, we focus on the Coulomb repulsion.

Figure 8 shows a momentum dependence of the charge susceptibility at the presence of Coulomb interactions. The parameters used were $q_0=0.8/a$ and $V=2$. Compared with a pure t-J model result in Fig. 4, one observes that $V_{\mathbf{q}}$ eliminates phase separation effects. We find also that small momentum divergences of the pairing fluctuations are suppressed also. However, Coulomb interaction effects are not significant at larger momenta. All the local correlation effects, which lead to a pronounced anisotropy of the charge susceptibility and its nontrivial doping dependence along the Γ-X direction, remain intact. As expected, the main effect of Coulomb interactions is to move potential charge instabilities to a finite momenta, as seen in Fig. 8. The divergence of $\chi_{\mathbf{q}}^{-1}$ at $q\to0$ corresponds to $\chi(\mathbf{q}=0)=0$, a well-known screening phenomenon in the presence of long-range Coulomb repulsion.

VI. APPLICATION: PHONON SOFTENING IN CUPRATES

Density fluctuations determine-doping induced phonon renormalization, as discussed earlier in a framework of
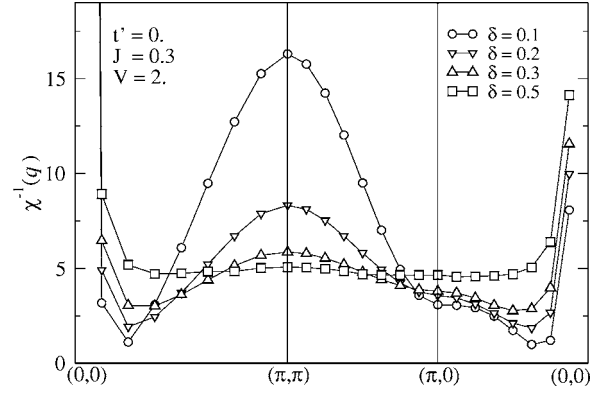

FIG. 8. Behavior of inverse charge susceptibility at $J=0.3$, $t'=0$. Coulomb repulsion with $V=2$, $\kappa=2/a$, and $q_0=0.8/a$ is included. Compare with Fig. 5.

slave-boson method,[19,20] and also by an exact diagonalization of small clusters.[40] In particular, a broad and anomalous line shape of the bond-streching phonons with momentum at $(\pi,0)$ direction has been found,[19] while no such anomalies were present for (π,π). The effect is strongly doping dependent.[20] We consider now how the phonon renormalization effects are modified when the pairing (pseudogap formation) is included. Specifically, we address here a phonon softening problem and discuss the results in the context of experimental reports.[2–4]

A doped hole couples to the bond-stretching vibrations of its four oxygen neighbors[19]

$$\mathcal{H}=g\sum_i n_i(u_x^i-u_{-x}^i+u_y^i-u_{-y}^i).\quad(42)$$

In a momentum space this reads as

$$\mathcal{H}=i\sqrt{E_b\omega_0}\sum_{\alpha,\mathbf{q}}\sin(q_\alpha a/2)(a_{\alpha,-\mathbf{q}}+a_{\alpha,\mathbf{q}}^\dagger)n_{\mathbf{q}}.\quad(43)$$

Here, $\alpha=x$ and y denotes the polarization of the oxygen displacement, and $\omega_0=\sqrt{K/m}$ is the phonon frequency determined by spring constant K and the oxygen mass m. Electron-phonon coupling strength is conveniently quantified by a binding energy

$$E_b=2g^2/K,\quad(44)$$

which would be gained in case of a static hole. By fitting a slave-boson theory to the experimental data on phonon softening and linewidth in cuprates, an estimation $E_b\sim t/2$ was obtained in Ref. 19.

We assume that the energies of density fluctuations are higher than the phonon energy—it should be valid not too close to charge instability. Within this assumption, we can use our static $\chi_{\mathbf{q}}$ to estimate phonon softening, $\delta\omega_{\mathbf{q}}=\omega_0-\omega_{\mathbf{q}}(\delta)$, which is obtained as follows:

$$\frac{\delta\omega_{\mathbf{q}}}{\omega_0}=1-\sqrt{1-2E_b\chi_{\mathbf{q}}(1-\gamma_{\mathbf{q}})}\simeq E_b\chi_{\mathbf{q}}(1-\gamma_{\mathbf{q}}),\quad(45)$$

where $\gamma_{\mathbf{q}}=(\cos q_x+\cos q_y)/2$ and $\chi_{\mathbf{q}}$ includes the Coulomb repulsion. Note also, that without correlations the product
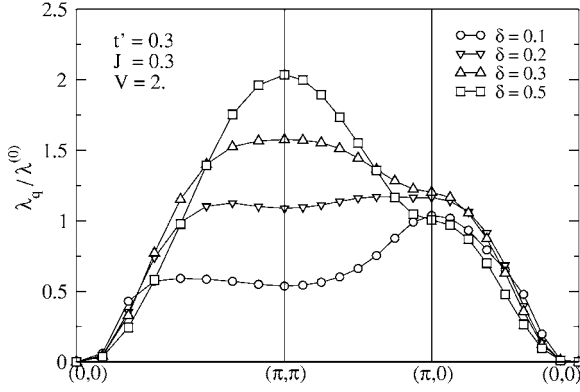
FIG. 9. Momentum dependence of the effective coupling constant [in units of the bare coupling $\lambda^{(0)}$] which determines the renormalization of the bond-stretching phonons. The parameters used were $t'=0.3$, $J=0.3$, $V=2$, and $\kappa=2/a$.

$E_b\chi_{\mathbf{q}}^{(0)}\simeq E_b/4t$. One can therefore introduce a dimensionless quantity $\lambda^{(0)}=E_b/4t$, which could be regarded as a "bare" coupling constant in the problem. According to Ref. 19, $\lambda^{(0)}\simeq 1/8$, justifying a perturbative treatment. Equation (45) reads now as

$$\delta\omega_{\mathbf{q}}/\omega_0 = \lambda_{\mathbf{q}} = \lambda^{(0)}4t\chi_{\mathbf{q}}(1-\gamma_{\mathbf{q}}). \qquad (46)$$

Factor $\gamma_{\mathbf{q}}$ in Eq. (46), which stems from the coupling geometry, would suggest a strongest softening for the full-breathing mode, that is, at $\mathbf{q}=(\pi,\pi)$. However, strong correlations change a momentum dependence of $\chi_{\mathbf{q}}$ dramatically by suppressing it at (π,π) and enhancing around $(\pi,0)$ points. One may say that correlations lead to the redistribution of the effective electron-phonon coupling in a momentum space. As a result, softening becomes strongest at $(\pi,0)$, consistent with experiment. This explanation of Ref. 19 is further supported by the present calculation, including the pseudogap and t' effects.

Figure 9 shows a general form of the renormalization factor $\lambda_{\mathbf{q}}/\lambda^{(0)}$ along particular directions in the Brillouin zone. This figure is in obvious correspondence with the above findings, and particularly, with Fig. 8.

Figure 10 presents more detailed doping dependence of $\lambda_{\mathbf{q}}/\lambda^{(0)}$ at $\mathbf{q}=(\pi,\pi)$ and $\mathbf{q}=(\pi,0)$. When multiplied by a bare constant $\lambda^{(0)}$, these curves correspond to the phonon softening $\delta\omega_{\mathbf{q}}/\omega_0$. As the latter is about 15–20% for $(\pi,0)$ phonon in optimally doped cuprates,[2,3] a bare constant $\lambda^{(0)}$ of the order of 0.15–0.20 is required to fit the observed data.[41] A striking similarity with the observed doping dependence[2,3] is worth pointing out here: both in experiment and in our theory, phonon softening along the $(\pi,0)$ direction is almost independent on doping in a wide region above $\delta\sim 0.12$. While such a trend was already found earlier,[20] J-pseudogap effects dramatically enhance the charge susceptibility along $(\pi,0)$ at small δ, hence it obtains nearly flat doping dependence rather unexpected in view of hole-dilution physics.

For further comparison of our theory with the available experimental data, we plot a momentum dependence of $\lambda_{\mathbf{q}}/\lambda^{(0)}$ along the Γ-X direction for several values of doping in Fig. 11. One finds that visible deviations from a simple
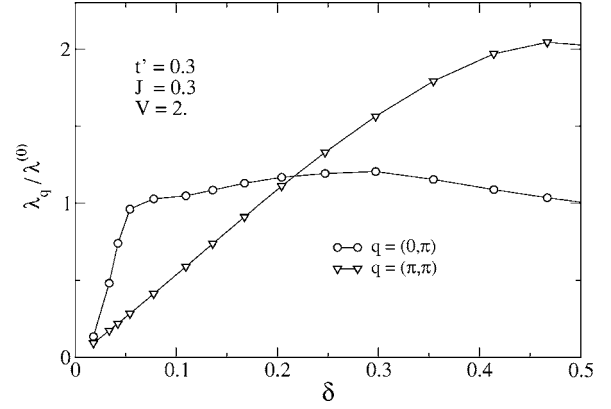

FIG. 10. Renormalization of phonons [in units of the bare coupling constant $\lambda^{(0)}$] at the symmetry points as a function of doping. The parameters used are as in Fig. 9.

cosine curve increase at smaller dopings, in general agreement with experiment.[3,4]

While present calculations do capture the most anomalous experimental findings—stronger and nonlinear doping effects along the $(\pi,0)$ direction—a quantitative comparison is much less satisfactory. In particular, a rather sharp kinklike change in doping dependence is observed in experiment at about $\delta\sim 0.12$,[2,3] while it is found in our theory at lower doping. One obvious reason for this discrepancy is that, strickly speaking, we cannot quantitatively address the phonon softening problem by using our *static* charge susceptibility. This is because the charge fluctuations for momenta along the $(\pi,0)$ direction extend to low energies (comparable to phonon ones), as shown both in a slave-boson theory[7] and in the numerical work.[9,10] A dynamical susceptibility is therefore required, which is, however, beyond the scope of present work. Yet another reason is that, focusing mainly on the pairing effects, we did not include an effective hopping contribution stemming from "Fock" decoupling of the J interaction. This contribution, which is a fraction of J/t,[5,7] will stabilize a Gutzwiller band-narrowing effect at doping levels $\sim(0.2$–$0.3)J/t$ below which a linear doping
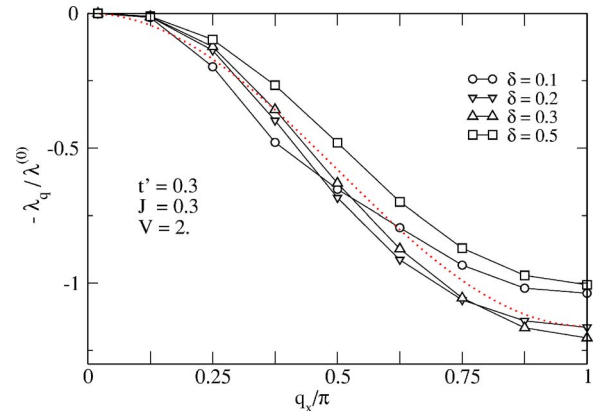

FIG. 11. (Color online) Renormalization of phonons along the $(0,\pi)$ direction [in units of $\lambda^{(0)}$]. The parameters used were $t'=0.3$, $J=0.3$, $V=2$, $\kappa=2/a$, and $q_0=0.8/a$. A simple cosine curve is shown for comparison by the dotted line.

dependence $\chi_{\tilde{q}} \propto \delta$ due to a hole-dilution effect sets in. This is expected to shift a kink feature to higher dopings as in experiment. Further, a quantitative description would also require the inclusion of spin-polaron effects beyond the leading $1/N$ approximation,[7,20] and a coupling of the charge fluctuations to a collective spin mode.[42]

In general, it seems that a kink feature in the doping dependence of $(\pi,0)$ phonon softening,[2,3] which apparently parallels with the so-called "Yamada plot" for the spin incommensurability,[43] provides an interesting test case for theory. Its initial linear behavior $\propto \delta$ is expected and can be explained in terms of sum rule arguments.[17] The saturation above a certain doping level is well captured by slave-boson theories, but it is not fully clear at present why such an abrupt regime change happens at around the "magic" doping $\sim 1/8$ concomitant with the saturation of spin incommensurability.

Finally, it is interesting to notice that the renormalization of density fluctuations and the so-called charge vertex $\gamma(k,q)$ of Refs. 12 and 13 [denoted by $\Gamma(p,q)$ in Refs. 15, 16, and 18] have a common origin. Reflecting this, the charge susceptibility can readily be expessed via $\gamma(k,q)$ [see, e.g., Eq. (16) of Ref. 13]. In fact, in case of zero frequency and small momenta one finds $\gamma(k_f, \mathbf{q}) \simeq \delta(\chi_{\mathbf{q}}/\chi_{\mathbf{q}}^{(0)})$. This relation clarifies the origin of strong momentum structure in the electron-phonon vertex function found in Refs. 12–16 and 18—this simply reflects the highly momentum-selective action of the Gutzwiller constraint on density fluctuations as we emphasized in previous sections of this paper. Indeed, as $\chi_{\mathbf{q}}/\chi_{\mathbf{q}}^{(0)} \propto 1/\delta$ at small momenta, one realizes that the effective electron-phonon interaction is essentially the bare one. At large momenta, however, it is strongly suppressed as the hole density δ is reduced.[44] This results in a "predominantly forward scattering" of electrons on phonons in cases when this coupling is located in a density channel (which is the case for the scattering on bond-stretching phonons). In the context of cuprates, one should, however, realize that this small-momentum peak structure in $\chi_{\mathbf{q}}$, hence also in $\gamma(k,q)$, is in fact suppressed by long-range Coulomb repulsion. Moreover, a bare matrix element for bond-stretching phonons is itself vanishing as q^2 at small $\mathbf{q}$ [observe the matrix elements $\sin(q_\alpha a/2)$ in Eq. (43) and the resulting the form-factor $(1-\gamma_{\mathbf{q}})$ in Eq. (45)]. These two factors eliminate the "forward-scattering" feature in cuprates. Altogether, it seems that effective coupling of the Fermi-surface electrons to bond-stretching phonons is somewhat reduced from $\lambda^{(0)}$ for both small and large values of momentum-transfer $\mathbf{q}$. Therefore, a significance of the bond-streching phonons for the electronic properties of doped cuprates should not be overemphasized.[44]

VII. CONCLUSIONS

We calculated a momentum dependence of the static charge susceptibility in the t-t'-J model at various doping levels. We employed the formalism, which effectively resums the RPA series in Gutzwiller, J term, and Coulomb repulsion V-channel simultaneously. We observe that $\chi(\mathbf{q})$ is

a featureless function in the limit of a weakly correlated overdoped regime. With decreasing of the doping level, strong correlations lead to a nontrivial, highly momentum-dependent renormalization effect that cannot be described in terms of simple hole-density dilution effects. We demonstrate that $\chi(\mathbf{q})$ is strongly suppressed near (π,π). However, $\chi(\mathbf{q})$ remains large around $(\pi,0)$ and $(0,\pi)$ regions even at dopings as small as 0.1–0.2. A strong anisotropy of charge dynamics at finite wave vectors has important experimental consequences, leading, e.g., to a pronounced anisotropy in a renormalization of the bond-stretching phonon modes as observed in cuprates. We find that the exchange J and second hopping t' influence the charge susceptibility in the opposite way—the former enhances it while t' and also Coulomb interactions weaken the small-momenta anomalies in $\chi(\mathbf{q})$. Implications of these findings on the spin and electronic properties deserve further analysis. The present study specifies the most "dangerous" regions in a momentum space where one may expect charge-related anomalies. A complex interplay between the charge, spin, and fermionic excitations should be considered to a fuller extent in order to locate more precisely a momentum position of low-energy charge modulations.

APPENDIX: COULOMB INTERACTION ON THE LATTICE: POINT-CHARGE LIMIT

Consider the formula for the Coulomb interaction (35) for $f(\mathbf{r}) = \delta(\mathbf{r})$. Introducing an auxiliary integration, the Fourier transform $V_{\mathbf{q}}$ at $q_z = 0$ can be written as

$$V_{\mathbf{q}} = \frac{V}{\pi^{3/2}} \int_0^\infty d\tau \sum_{\mathbf{r}_i \neq 0} e^{-\tau^2(r_i^2 + \tilde{z}_i^2) + i\mathbf{q}\mathbf{r}}, \qquad (A1)$$

where $r_i^2 = x_i^2 + y_i^2$ denote square lattice sites with $x_i, y_i = (0, \pm 1, \pm 2, \ldots)$, while $\tilde{z}_i = (0, \pm 1, \pm 2, \ldots)\tilde{d}$; we set $a = 1$ here. We use now the definition of the Jacobi ϑ function

$$\vartheta_3(u,q) = \sum_{n=-\infty}^\infty q^{-n^2} e^{2iun}$$

and represent Eq. (A1) in the form

$$V_{\mathbf{q}} = \frac{V}{\pi^{3/2}} \int_0^\infty d\tau \left[\varphi\left(\frac{\mathbf{q}}{2}, e^{-\tau^2}\right) - 1 \right], \qquad (A2)$$

$$\varphi(\mathbf{q},s) = \vartheta_3(q_x,s)\vartheta_3(q_y,s)\vartheta_3(0,s^{\tilde{d}^2}). \qquad (A3)$$

This formula can be considered as the limiting case of Eq. (38) with $\kappa \to \infty$. Numerically, the values of $V_{\mathbf{q}}$ in the whole Brillouin zone given by Eqs. (38) and (A2) become very close at $\kappa \gtrsim 3$.

*On leave from Petersburg Nuclear Physics Institute, Gatchina 188300, Russia.

[1] T. Hanaguri, C. Lupien, Y. Kohsaka, D.-H. Lee, M. Azuma, M. Takano, H. Takagi, and J. C. Davis, Nature (London) **430**, 1001 (2004).

[2] L. Pintschovius, Phys. Status Solidi B **242**, 30 (2005).

[3] T. Fukuda, J. Mizuki, K. Ikeuchi, K. Yamada, A. Q. R. Baron, and S. Tsutsui, Phys. Rev. B **71**, 060501(R) (2005).

[4] D. Reznik, L. Pintschovius, M. Ito, S. Iikubo, M. Sato, H. Goka, M. Fujita, K. Yamada, G. D. Gu, and J. M. Tranquada, Nature (London) **440**, 1170 (2006).

[5] Z. Wang, Y. Bang, and G. Kotliar, Phys. Rev. Lett. **67**, 2733 (1991).

[6] L. Gehlhoff and R. Zeyher, Phys. Rev. B **52**, 4635 (1995).

[7] G. Khaliullin and P. Horsch, Phys. Rev. B **54**, R9600 (1996).

[8] W. Zimmermann, R. Frésard, and P. Wölfle, Phys. Rev. B **56**, 10097 (1997).

[9] T. Tohyama, P. Horsch, and S. Maekawa, Phys. Rev. Lett. **74**, 980 (1995).

[10] R. Eder, Y. Ohta, and S. Maekawa, Phys. Rev. Lett. **74**, 5124 (1995).

[11] J. H. Kim, K. Levin, R. Wentzcovitch, and A. Auerbach, Phys. Rev. B **44**, 5148 (1991).

[12] M. L. Kulić and R. Zeyher, Phys. Rev. B **49**, 4395 (1994); R. Zeyher and M. L. Kulić, *ibid.* **53**, 2850 (1996).

[13] R. Zeyher and M. L. Kulić, Phys. Rev. B **54**, 8985 (1996).

[14] F. Becca, M. Tarquini, M. Grilli, and C. Di Castro, Phys. Rev. B **54**, 12443 (1996).

[15] E. Koch and R. Zeyher, Phys. Rev. B **70**, 094510 (2004).

[16] Z. B. Huang, W. Hanke, E. Arrigoni, and D. J. Scalapino, Phys. Rev. B **68**, 220507(R) (2003).

[17] O. Rösch and O. Gunnarsson, Phys. Rev. Lett. **93**, 237001 (2004).

[18] R. Citro, S. Cojocaru, and M. Marinaro, Phys. Rev. B **72**, 115108 (2005).

[19] G. Khaliullin and P. Horsch, Physica C **282-287**, 1751 (1997).

[20] P. Horsch and G. Khaliullin, Physica B **359-361**, 620 (2005).

[21] N. Furukawa and M. Imada, J. Phys. Soc. Jpn. **61**, 3331 (1992).

[22] M. Kohno, Phys. Rev. B **55**, 1435 (1997).

[23] A. Tandon, Z. Wang, and G. Kotliar, Phys. Rev. Lett. **83**, 2046 (1999).

[24] R. H. McKenzie, J. Merino, J. B. Marston, and O. P. Sushkov, Phys. Rev. B **64**, 085109 (2001).

[25] C. S. Hellberg and E. Manousakis, Phys. Rev. Lett. **78**, 4609 (1997); see also E. Dagotto, Rev. Mod. Phys. **66**, 763 (1994), and references therein.

[26] M. Deeg and H. Fehske, Phys. Rev. B **50**, 17874 (1994).

[27] A question as to whether the compressibility is truly divergent is somewhat controversial: e.g., F. Becca, M. Capone, and S. Sorella [Phys. Rev. B **62**, 12700 (2000)] argue that the ground state is uniform.

[28] S. Winterfeldt and D. Ihle, Phys. Rev. B **58**, 9402 (1998).

[29] A. Larkin and A. Varlamov, in *Theory of Fluctuations in Superconductors*, International Series of Monographs on Physics 127 (Oxford University Press, New York, 2005); see also cond-mat/0109177.

[30] M. Vojta and S. Sachdev, Phys. Rev. Lett. **83**, 3916 (1999).

[31] M. Vojta, Y. Zhang, and S. Sachdev, Phys. Rev. B **62**, 6721 (2000); M. Vojta, *ibid.* **66**, 104505 (2002).

[32] E. Pavarini, I. Dasgupta, T. Saha-Dasgupta, O. Jepsen, and O. K. Andersen, Phys. Rev. Lett. **87**, 047003 (2001).

[33] T. Tohyama, Phys. Rev. B **70**, 174517 (2004).

[34] V. N. Kotov and O. P. Sushkov, Phys. Rev. B **70**, 195105 (2004).

[35] S. R. White and D. J. Scalapino, Phys. Rev. B **60**, R753 (1999).

[36] D. Reagor, E. Ahrens, S.-W. Cheong, A. Migliori, and Z. Fisk, Phys. Rev. Lett. **62**, 2048 (1989).

[37] A. L. Fetter, Ann. Phys. (N.Y.) **88**, 1 (1974).

[38] We note in passing that the present model estimates the in-plane plasma frequency as $\omega_p \simeq \sqrt{V_\infty t \delta}$, where $V_\infty = 4\pi e^2/d\epsilon_\infty$. With a high-frequency screening constant $\epsilon_\infty \simeq 5$, (Ref. 36) and $t = 0.43$ eV, (Ref. 32) this gives $\omega_p \simeq 0.7$ eV at $\delta = 0.2$, close to the observed value ~ 0.8 eV (Ref. 39).

[39] S. Uchida, T. Ido, H. Takagi, T. Arima, Y. Tokura, and S. Tajima, Phys. Rev. B **43**, 7942 (1991).

[40] O. Rösch and O. Gunnarsson, Phys. Rev. Lett. **92**, 146403 (2004).

[41] A smallness of this constant might seem surprising in view of the strong anticipated change of the Zhang-Rice singlet energy by oxygen displacements. However, a doped-hole wave function is rather extended and made predominantly of the oxygen orbitals (Ref. 32). Hence, the energy modulation by displacement of the oxygen sites themselves could be not very large. In fact, LDA calculations show that this coupling is indeed rather weak (see S. Y. Savrasov and O. K. Andersen, Phys. Rev. Lett. **77**, 4430 (1996); O. K. Andersen, S. Y. Savrasov, O. Jepsen, and A. I. Liechtenstein, J. Low Temp. Phys. **105**, 285 (1996)).

[42] P. Horsch and G. Khaliullin (unpublished).

[43] K. Yamada, C. H. Lee, K. Kurahashi, J. Wada, S. Wakimoto, S. Ueki, H. Kimura, Y. Endoh, S. Hosoya, G. Shirane, R. J. Birgeneau, M. Greven, M. A. Kastner, and Y. J. Kim, Phys. Rev. B **57**, 6165 (1998).

[44] These findings are related to the scattering of electrons in a metallic phase when a large Fermi-surface is formed. A single-hole problem is radically different: in that case, correlations may considerably enhance the electron-phonon coupling constant, see, e.g., A. Ramšak, P. Horsch, and P. Fulde, Phys. Rev. B **46**, 14305 (1992); A. S. Mishchenko and N. Nagaosa, Phys. Rev. Lett. **93**, 036402 (2004). Moreover, the bare coupling constant for a single-hole in insulator is itself different (larger and non-local) since no metallic screening of the doped charge is present in that case.